TIDAL EFFECTS IN EXCURSION SET BASED MODELS OF GRAVITATIONAL COLLAPSE

Haritha R

MS12117

A dissertation submitted for the partial fulfilment of

BS-MS dual degree in Science

Indian Institute of Science Education and Research Mohali

April 2017

Certificate of Examination

This is to certify that the dissertation titled **"Tidal effects in Excursion set based models of Gravitational collapse"** submitted by **Haritha. R** (Reg. No. MS12117) for the partial fulfillment of BS-MS dual degree program of the Institute, has been examined by the thesis committee duly appointed by the Institute. The committee finds the work done by the candidate satisfactory and recommends that the report be accepted.

Prof. Sudeshna Sinha Dr. H K Jassal Prof. Jasjeet Singh Bagla

(Supervisor)

Dated:

Declaration

The work presented in this dissertation has been carried out by me under the guidance of Prof. Jasjeet Singh Bagla at the Indian Institute of Science Education and Research Mohali.

This work has not been submitted in part or in full for a degree, a diploma, or a fellowship to any other university or institute. Whenever contributions of others are involved, every effort is made to indicate this clearly, with due acknowledgement of collaborative research and discussions. This thesis is a bonafide record of original work done by me and all sources listed within have been detailed in the bibliography.

Haritha R

MS12117

Dated: April 21, 2017

In my capacity as the supervisor of the candidate's project work, I certify that the above statements by the candidate are true to the best of my knowledge.

Prof. Jasjeet Singh Bagla

(Thesis Supervisor).

Acknowledgements

First and foremost, I would like to thank my thesis supervisor Prof. Jasjeet Singh Bagla, without whose help and supervision, this thesis would have never been possible. The discussions that I had with him has enhanced my capabilities at a professional level. Also I would like to thank my thesis committee members Prof. Sudeshna Sinha and Dr. Harvinder Kaur Jassal for their valuable suggestions and criticism of my work.

I owe my deepest gratitude to Sandeep Rana for helping me with the discussions. I am grateful to Dr. Smriti Mahajan for conducting Astro Journal Club actively, and also to other members of the club.

I am highly grateful to the Deputy Librarian, Dr. Vishaki, Library Information Assistant Mr. Shameer K. K. for their promptness and assistance.

I would like to thank all my friends for supporting and helping me during the entire period of the project. I am thankful also to my seniors for their useful advice and help. I would like to acknowledge the moral support and encouragement, that I have received from my parents and brother.

Finally, I am thankful to IISER Mohali for providing me Infrastructure and Computer Centre for all the technical support. I would like to acknowledge DST INSPIRE, Government of India for the financial support.

Haritha R

List of Figures

2.1 Amplitude of density contrast vs scale 9

2.2 Density vs scale factor for spherical collapse 12

2.3 Evolution of ellipsoidal perturbations in an Einstein-de Sitter universe 18

2.4 δ_{ec}/δ_{sc} and σ/σ_* as a function of γ 20

2.5 Improvement in estimated halo mass of ellipsoidal collapse as compared to spherical collapse 21

3.1 Δ^2_δ vs k 28

3.2 Spectral parameter γ vs $\frac{R_0}{R_1}$ for ΛCDM model 29

3.3 Spectral parameter γ vs $\frac{R_0}{R_1}$ for $n = 0$ 30

3.4 Spectral parameter γ vs $\frac{R_0}{R_1}$ for $n = -1$ 30

3.5 Spectral parameter γ vs $\frac{R_0}{R_1}$ for $n = -2$ 31

Contents

Abstract **v**

1 Introduction **1**

2 Gravitational collapse **3**

2.1 Linear theory 3

2.1.1 Background informations 3

2.1.2 Equations of motion 6

2.2 Gaussian random fields 9

2.3 Spherical collapse 10

2.3.1 Press-Schechter theory 13

2.4 Correlation function and Power Spectrum 14

2.5 Power spectrum of density fluctuation 15

2.6 Ellipsoidal collapse 15

2.6.1 Zel'dovich approximation 15

2.6.2 Extended Press-Schechter theory 17

3 Environmental dependence **23**

3.1 Smoothing of fields 23

3.2 Basic concepts 25

3.2.1 Environmental effect from the initial shear 26

4 Conclusions **33**

Abstract

Gravitation plays a major role in the formation of bounded objects in the universe [15]. For their formation, virialized objects had to overcome the expansion of universe. This can be easily done if they grow from initial overdensities. If we have a model for gravitational collapse, the abundance of virialized objects can give information about the initial fluctuation spectrum. Almost all bounded objects like stars are formed inside collapsed, virialized dark matter halos which are condensed out of these initial density fluctuations. Current models of structure formation work with the assumption that structure formation happens hierarchically from small, initial Gaussian density fluctuations. Formation of dark matter halos and their properties can be studied using N-body simulations as well as analytical models. An important prediction that one can have from hierarchical structure formation is the mass function: i.e., the number density of objects as a function of their mass, M. Shape and evolution of the mass function of bound objects can be predicted using Press-Schechter and Excursion set approach. But the predicted mass function from these models is accurate only at the high mass end. It has been shown that this discrepancy between theory and simulation can be reduced if bound structures are assumed to form from an ellipsoidal rather than from a spherical collapse. In the case of an ellipsoidal collapse, there is an effect of environment on the halos from the local shear, which is not relevant in spherical collapse model [22].

Chapter 1

Introduction

Current galaxy formation models work with the assumption that the gravitational clustering is due to density perturbations in the initial density field. Low mass halos are formed at the early stages, and these merge and accrete mass to grow into large gravitationally bounded dark matter halos. Objects like stars and galaxies are formed in these halos as the gas inside it cools down [1]; [2]; [3]. If we need to study the evolution of these objects, it is essential to study the properties of dark matter halos [4]. Among them, an important property is the halo mass function. It gives the number density of dark matter halos as a function of mass, $n(M)$ [5].

$$n(M)dM = \frac{\bar{\rho}}{M}\left|\frac{dF}{dM}\right|dM \tag{1.1}$$

where $|dF/dM|$ is the fraction of volume occupied by virialized halos having mass in between M and $M+dM$ [6]. First model of mass function was proposed by Press and Schechter [7]. Press-Schechter approach can be related to the concept of random walks [19]. But the mass function calculated using theory and simulation do not match for low mass halos. This model under predicted high mass halos and over predicted low mass halos. This discrepancy is not surprising since some approximations are used in this model that may not be valid. In particular, the perturbations in Gaussian random fields [1] are inherently triaxial. By introducing ellipsoidal collapse, these discrepancies were reduced [15].

Press and Schechter (1974) argued that collapsed halos at a late time can be identified by looking at the initial density field. Bond et al. (1991) work with the assumption

[1] we will introduce Gaussian random fields in section 2.2

that objects form by spherical collapse, this assumption may be combined with assumption that the initial density fluctuation was a Gaussian random field. Main assumption that they use is: (i) collapse of a region happens when the initial overdensity within the region exceeds a critical value, δ_{sc} and this critical value depends only on time, not the initial size of the region.

Even though this spherical approximation works well for initial collapse, it is not accurate since perturbations in the Gaussian density fields are inherently triaxial [20]. Here in the formation of non-linear structures, shear field plays a major role. In ellipsoidal collapse model, the evolution of the triaxial perturbation is influenced by large-scale tidal shear. In case of [8], in the linear regime, the initial conditions and external tides are chosen to recover Zel'dovich approximation. According to [15], including non-sphericity introduces a mass dependence on critical collapse density. Hence the introduction of ellipsoidal dynamics in the theory of mass function must take into account the environmental effect because of the tidal field generated by the large scale environment.

In this report, we compare spherical and ellipsoidal collapse models: how the models work and how the halo and environment are connected. In the first part we start by introducing the linear theory, how it works. After that we introduce two models to calculate dark matter halo mass functions (Press-Schechter and Extended Press-Schechter). In the last part, we study the effect of environment on halos using specific examples for power spectrum.

Chapter 2

Gravitational collapse

2.1 Linear theory

2.1.1 Background informations

Comoving Coordinates

Comoving distance and Proper distance are the two measures used in cosmology. Proper distance, $\mathbf{r}(t)$ is the physical distance to the present location of a distant object. This distance can change over time due to expansion of the universe. The comoving distance, $\mathbf{x}(t)$ is defined such that it does not change over time due to the expansion of the universe. These are related as follows:

$$\mathbf{r}(t) = a(t)\mathbf{x} \tag{2.1}$$

where $a(t)$ is the scale factor that describes the expansion of the universe, $\mathbf{r}$ is the physical coordinate which gives the location and $\mathbf{x}$ is the comoving position of the object in consideration. For the present epoch, $a(t)$ is chosen so that $a(t_0) = a_0 = 1$. The universe we are considering here is the FLRW (Friedmann-Lemaitre-Robertson-Walker) universe and it refers to an isotropic and homogeneous, expanding or contracting universe [16]. These are solutions of Einstein's field equations of General Theory of Relativity [10].

Density perturbations

Perturbations are present in various physical quantities. We will focus on perturbations in density $\rho(\mathbf{r}, t)$, where $\mathbf{r}$ gives the location. Let us denote the background density of the universe as $\bar{\rho}(t)$ and the local density as $\rho(\mathbf{r}, t)$. In an unperturbed universe, value of the density will be the same at all points. Density perturbation in comoving and physical coordinates can be defined using the equation

$$\delta(\mathbf{x}, t) \equiv \frac{\rho(\mathbf{x}, t) - \bar{\rho}(t)}{\bar{\rho}(t)}. \tag{2.2}$$

Studying the growth of δ, we can have an idea regarding the formation and evolution of collapsed structures. In an unperturbed universe where $\rho(\mathbf{r}, t) = \bar{\rho}(t)$, $\delta(\mathbf{x}, t) = 0$. Density contrast can be positive or negative. In the first case, density contrast can grow limitless. There is nothing to prevent this. But in case of negative fluctuations, there is a boundary. We can't go below $\delta = -1$. Because, something emptier than empty does not exist.

Density perturbations in different components of the universe behave differently. Radiation, baryonic matter, dark matter and dark energy are some of the components and each of them has its own evolution. Hence we can say that total density $\rho(\mathbf{r}, t)$ in the universe is the subtotal of all components and it can be written as:

$$\rho(\mathbf{r}, t) = \rho_{DM}(\mathbf{r}, t) + \rho_{rad}(\mathbf{r}, t) + \rho_B(\mathbf{r}, t) + \rho_{DE}(\mathbf{r}, t). \tag{2.3}$$

But we generally consider the contribution from the dominant components and by combining the matter components together, this equation (2.3) will become $\rho_m = \rho_B + \rho_{DM}$, where B is for Baryons.

Pressure perturbations

Pressure gradients due to perturbations have great influence on the evolution of perturbations in the early universe. The idea of gravitational instability plays a major role in the growth of density perturbations. Pressure perturbations travel as sound waves. Total pressure has three major components. From baryonic matter, radiation and dark energy. Dark matter is non-relativistic and hence its pressure can be ignored. The total pressure can be written as:

$$P(\mathbf{r}, t) = P_B(\mathbf{r}, t) + P_{rad}(\mathbf{r}, t) + P_{DE}(\mathbf{r}, t). \tag{2.4}$$

Since dark energy is not expected to have significant perturbations at small scale, contribution to pressure gradient comes from radiation and baryonic matter. Radiation is subdominant at $z \ll 10^3$ and baryons also constitute only 4.5% of the total energy density. Hence pressure perturbations may be ignored to first order.

Velocity perturbations

We know that, in an FLRW universe, everything moves with Hubble expansion and it is described by Hubble parameter, $H(t)$

$$H(t) = \frac{\dot{a}}{a} \tag{2.5}$$

and it has Hubble velocity, $\mathbf{v}_H(\mathbf{r})$ given by

$$\mathbf{v}_H(\mathbf{r}) = H(t)\mathbf{r}. \tag{2.6}$$

There is an additional component of velocity called peculiar velocity, $\mathbf{v}$. Hence the total velocity, $\mathbf{u}$ of an object can be written as

$$\mathbf{u}(\mathbf{r}, t) = \mathbf{v}_H(\mathbf{x}, t) + \mathbf{v}(\mathbf{x}, t). \tag{2.7}$$

We have taken $\mathbf{r} = a(t)\mathbf{x}(t)$. We can write

$$\mathbf{u} = \frac{d\mathbf{r}}{dt} = \dot{a}\mathbf{x} + a\dot{\mathbf{x}} = \mathbf{v}_H(\mathbf{x}, t) + a(t)\dot{\mathbf{x}}. \tag{2.8}$$

From here, we have an expression for peculiar velocity:

$$\mathbf{v} = a(t)\dot{\mathbf{x}}. \tag{2.9}$$

Potential perturbations

Potential and density are related via Poisson equation and hence density perturbation imply perturbations in the gravitational potential Φ. In general, we need to consider the contribution from matter, radiation and dark energy. Here we are considering the field due to radiation to be weak. In the Newtonian limit:

$$\nabla_r^2(\Phi) = 4\pi G\left(\rho(\mathbf{r}, t) + \frac{3P}{c^2}\right). \tag{2.10}$$

In case of matter dominated universe, we can neglect the pressure, however dark energy contributes a pressure term. Here the background potential is denoted by Φ_u where

$$\Phi_u = \frac{1}{2}\ddot{a}\mathbf{x}^2. \tag{2.11}$$

The potential get contribution from different components and the potential perturbation ϕ is given by the equation

$$\phi(\mathbf{x}, t) = \Phi(\mathbf{r}, t) - \frac{1}{2} a\ddot{a}\mathbf{x}^2 \tag{2.12}$$

and the Poisson equation is

$$\nabla^2\phi = 4\pi G\bar{\rho}a^2\delta. \tag{2.13}$$

2.1.2 Equations of motion

Using the background information from section (2.1.1), we can fully describe the evolution of structures in the universe. When we are studying the formation of structures on large scales ($r \gg 1pc$), we may consider the matter as a continuous fluid. The evolution of the fluid can be described in terms of three main fluid equations.
The **Continuity equation** which describes the conservation of mass, **Euler equation** which gives the acceleration of the fluid element due to gravitational force and pressure gradients in the fluid and finally the **Poisson equation** which gives the gravitational potential. Also required is the **Equation of state**: the relation between density and pressure. The following calculations have been done for a matter dominated universe in physical coordinates. The quantities are density $\rho(\mathbf{r}, t)$ at a point $\mathbf{r}$, total velocity $\mathbf{u}(\mathbf{r}, t)$, total gravitational potential $\Phi(\mathbf{r})$ and pressure of the medium, $P(\mathbf{r}, t)$ (refer to [9], [10]).

Continuity equation

Continuity equation gives the idea of conservation of mass. According to this equation, the growth of mass in a volume is equal to the net amount of matter flowing in (total flux). In the case of a non-relativistic matter component we have,

$$\frac{\partial\rho}{\partial t} + \nabla_r . \rho\mathbf{u} = 0. \tag{2.14}$$

As we can see, equation (2.14) connects the density of the medium $\rho(\mathbf{r}, t)$ and velocity of the flow $\mathbf{u}(\mathbf{r}, t)$.

Euler's equation

Euler's equation is the equation of motion for ideal fluids which includes gravitational force as well as force due to pressure gradients in the medium.

$$\frac{\partial \mathbf{u}}{\partial t} + (\mathbf{u}.\nabla_r)\,\mathbf{u} = -\frac{1}{\rho}\nabla_r P - \nabla_r \Phi. \tag{2.15}$$

Equation of state

The pressure exerted by a medium usually depends on the density and entropy of the medium and is given by the equation of the state,

$$P = P(\rho, S) \tag{2.16}$$

where S is the entropy of the medium. Each constituent of the universe can be modeled as a barotropic fluid, i.e., the contribution from different components in the universe is given by the a constant w,

$$P(\rho) = w\rho c^2 \tag{2.17}$$

where c is the speed of light. In case of matter, pressure is negligible and hence $w_m = 0$. But in case of radiation, $w_{rad} = 1/3$ and for dark energy, $-1 < w_{DE} < -1/3$.
If there are no perturbations, the solution of the equations (2.14), and (2.15) is

$$\bar{\rho} \propto a^{-3}, \mathbf{u} = \frac{\dot{a}}{a}\mathbf{r}, \bar{\Phi} = \frac{2\pi G}{3}\bar{\rho}\mathbf{r}^2. \tag{2.18}$$

If we consider perturbations then,

$$\rho = \bar{\rho} + \rho\delta, \mathbf{u} = H\mathbf{r} + \mathbf{v}, \Phi = \bar{\Phi} + \phi \tag{2.19}$$

Where δ is the density contrast and H is the Hubble's constant. We have already defined the comoving coordinate $\mathbf{x} = \mathbf{r}/a(t)$ and proper time, $d\tau = dt/a$. Substituting these back in the equation, we get the following set of equations where all the derivatives are now in terms of τ and $\mathbf{x}$:

$$\dot{\delta} + \nabla.\left((1+\delta)\,\mathbf{v}\right) = 0, \tag{2.20}$$

$$\frac{d\mathbf{v}}{dt} = -\frac{\dot{a}}{a}\mathbf{v} - \frac{1}{\rho}\nabla P - \nabla\phi, \tag{2.21}$$

and

$$\nabla^2\phi = 4\pi G\bar{\rho}a^2\delta. \tag{2.22}$$

We can linearize the above equations when perturbations are very small. We get:

$$\dot{\delta} + \nabla \mathbf{v} = 0. \tag{2.23}$$

Combining the equations (2.20) − (2.22), we get the following equation for density contrast:

$$\frac{d^2\delta}{dt^2} + 2\frac{\dot{a}}{a}\frac{d\delta}{dt} = 4\pi G\bar{\rho}\delta + \frac{1}{a^2}c_s^2\nabla^2\delta \tag{2.24}$$

where $c_s = \sqrt{dP/d\rho}$ is the speed of sound. In equation (2.24), the second term on the left-hand side is the damping term due to expansion of the universe, first term on the right-hand side is the gravitational driving term and the second term on the right denotes the pressure support.

Let us decompose δ in terms of plain wave modes, $\delta(\mathbf{x}, t) = \sum \delta_k e^{i\mathbf{x}.k}$ where we define $\lambda = 2\pi a/k$ in the physical coordinates. At large scales, gravity dominates whereas at small scales, pressure is more important. When the scale exceeds Jeans scale, the perturbation is unstable and Jeans scale is given by, $\lambda_J = c_s\sqrt{\pi/G\rho_0}$, where G is Newton's gravitational constant. In case of dark matter, the matter pressure term vanishes and equation (2.24) takes the form

$$\frac{d^2\delta}{dt^2} + 2\frac{\dot{a}}{a}\frac{d\delta}{dt} = 4\pi G\bar{\rho}\delta. \tag{2.25}$$

Consider an Einstein-de Sitter universe where $\Omega_m = 1$, the scale factor grows as $a \propto t^{2/3}$ and $\rho = \rho_m \propto a^{-3}$. There are two solutions for equation (2.25), these are: $\delta \propto t^{2/3}$ and $\delta \propto t^{-1}$. In a model with the cosmological constant, this dominates over matter at late times and the the solution is $\delta \approx$ constant.

We can say that, the density contrast grows as $t^{2/3}$ during the matter dominated era. Figure 2.1 gives the variation in density fluctuation with scale. Linear theory breaks when the fluctuations are large enough such that $\delta \simeq 1$. In this regime, equations (2.14) and (2.15) can't be solved analytically for general initial conditions and we need numerical simulations.

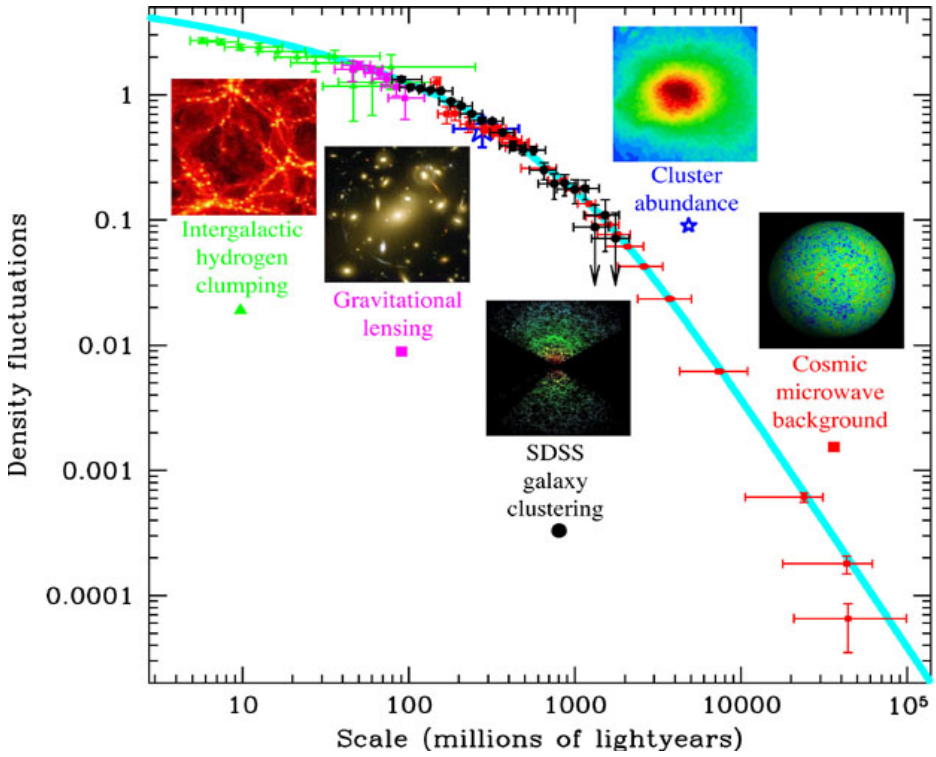

Figure 2.1: Data points give the power spectrum measurements, and blue curve gives the theoretical predictions for the amplitude of density fluctuations as a function of scale [11].

2.2 Gaussian random fields

Random fields and processes are common in Astronomy. The distribution of stars and galaxies, distribution of disturbances in the sun, the distribution of electrons in a CCD image; all are random processes. In astronomy, we use statistics to describe these processes. Random field is actually a stochastic process which takes values in a Euclidean space and is defined in a parameter space of dimensionality at least one. Almost all models of structure formation work with the assumption that initial fluctuations generated during the time of inflation constitute a Gaussian random field. A one-point Gaussian probability distribution function is the most fundamental distribution function[9] and is defined as the probability at any point inside a volume with a value $Y_c = [y, y+dy]$ where Y_G is a Gaussian stochastic process with the average value y_c and dispersion σ. Then the probability for the process $Y_G = [y, y + dy]$ is

given by

$$P(y)dy = \frac{1}{\sqrt{2\pi}\sigma}\exp -\frac{(y-y_c)^2}{2\sigma^2}dy. \tag{2.26}$$

When this process concerns an entire region of the space, it leads to the idea of a Gaussian Random field. In a homogeneous Gaussian random field, the probability at any one location in a volume with the value $Y_G = [y, y+dy]$ is given by the one-point Gaussian distribution in the equation (2.26). Also in case of a Gaussian random field, there will be questions regarding the probability of the field at X_1 with a value $Y(x_1) = y_1$, at X_2, a value $Y(x_2) = y_2$, and so on for n points, i.e., $Y(x_n) = y_n$ at X_n. Here, two-point probability distribution function, $P(y_1 y_2)$,

$$P(y_1y_2)dy_1dy_2 = \frac{1}{(2\pi)(\sqrt{detM})}exp\left[-\begin{pmatrix} y_1 & y_2 \end{pmatrix} M^{-1}\begin{pmatrix} y_1 \\ y_2 \end{pmatrix}/2\right]dy_1dy_2 \tag{2.27}$$

where M^{-1} is the inverse of the correlation matrix M,

$$M = \begin{pmatrix} \xi(0) & \xi(y_1y_2) \\ \xi(y_1y_2) & \xi(0) \end{pmatrix} = \begin{pmatrix} \sigma^2 & \xi(r) \\ \xi(r) & \sigma^2 \end{pmatrix} \tag{2.28}$$

with ξ as the correlation function. A random field in general requires all the n-point probability distributions for a complete description. If the distribution is Gaussian, this means

$$P(y_1,...,y_2)dy_1..dy_n = \frac{1}{(2\pi)(\sqrt{detM})}exp\left[-\begin{pmatrix} y_1,...,y_2 \end{pmatrix} M^{-1}\begin{pmatrix} y_1 \\ ... \\ y_2 \end{pmatrix}/2\right]dy_1,...,dy_n. \tag{2.29}$$

2.3 Spherical collapse

Gravitational instability and resulting collapse is the primary mechanism for structure formation in the universe. Gravitational instability is collapsed under the influence of self-gravity, where matter falls towards the center of mass. Spherical collapse model is the simplest model for the formation of non-linear, gravitationally bound structures. Imagine a spherical region with density higher than the density of the background in an Einstein-de Sitter universe. According to general theory of relativity, evolution of a spherical overdensity is independent of the background evolution and it evolves

like a sub-universe with the local density guiding the evolution. In other words, the evolution of a spherical density perturbation is identical to the evolution of the universe with a matter density equal to the density of the initial perturbation. If we have a spherical perturbation, then in the Newtonian limit,

$$\frac{d^2r}{dt^2} = -\frac{GM}{r^2}. \tag{2.30}$$

Where M is the mass contained in the sphere and r is the radius of the sphere. Multiplying by $\dot{r}$ and integrating the above equation, we have

$$\dot{r}^2 = \frac{2GM}{r} + C. \tag{2.31}$$

Equation (2.31) gives the first integral and is related to energy [12]. This equation has the following parametric solution;

$$r = A(1 - \cos\theta) \tag{2.32}$$

$$t = B(\theta - \sin\theta) \tag{2.33}$$

where θ is a parameter. The constants A and B are given by

$$A = \frac{\Omega_{m0}}{2(\Omega_{m0} - 1)} \tag{2.34}$$

$$B = \frac{\Omega_{m0}}{2H_0(\Omega_{m0} - 1)^{3/2}} \tag{2.35}$$

where $\Omega_{m0} > 1$ is the density parameter of the universe and H_0 is the Hubble's constant. We study the behavior of the system at early times. Perturbation initially expands with the Hubble's flow. For $\theta \to 0$, $r = A\theta^2/2$ and $t = B\theta^3/6$. Hence $\theta^6 = 8r^3/A^3 = 36t^2/B^2$, or $r^3 = (9/2)GMt^2$. Now $r^3 = 3M/4\pi\rho$, so we get $6\pi G\rho = t^2$. In order to relate this to the overall cosmic expansion, we have $H^2 = 8\pi G\rho/3$ and $6\pi G\rho = (9/4)H^2$ and we get $(9/4)H^2 = t^2$ or $t = 2/3H$. This is exactly the time evolution of an Einstein-de Sitter universe. At early times when θ is small, our spherical model evolves like a $\Omega = 1$ universe. The initial mass of the system is $M = 4\pi\bar{\rho}r^3/3$. If the density is enhanced by a factor δ, radius must shrink (by δr) in order to conserve the enclosed mass:

$$M = \frac{4\pi}{3}\bar{\rho}(1 + \delta)(1 + \delta r)^3. \tag{2.36}$$

Equating the initial and final masses gives $(1+\delta)(1+\delta r)^3 = 1$. Expanding to first order leads to

$$\delta \approx -3\delta r = \pm\frac{3}{20}\left(\frac{6t}{B}\right)^{2/3} \tag{2.37}$$

We can use these formulas to explain the events in the perturbation's history. In the initial phase, it is undergoing Hubble expansion. Then it breaks away due to self gravity and reaches a maximum radius at $\theta = \pi$; i.e., $r = 2A$ and $t = \pi B$. Final collapse occurs when $\theta = 2\pi$, $r = 0$, and $t = 2\pi B = 2t_{TA}$. Hence we can estimate the linearly extrapolated density contrast at turnaround and collapse as:

$$\delta_{turnaround} = (3/20)(6\pi)^{2/3} = 1.06 \tag{2.38}$$

$$\delta_{collapse} = (3/20)(12\pi)^{2/3} = 1.69. \tag{2.39}$$

When linearly evolved density contrast of a perturbation exceeds unity, it turns around and begins to contract. The corresponding number for collapse is 1.69.

The point at which expansion stops is defined as the time of turn-around. In the non-linear solution, we have

$$(1+\delta_{TA}) = \frac{9\pi^2}{16} = 5.55. \tag{2.40}$$

The collapsing phase leads to virial equilibrium. In realistic perturbations, deviations

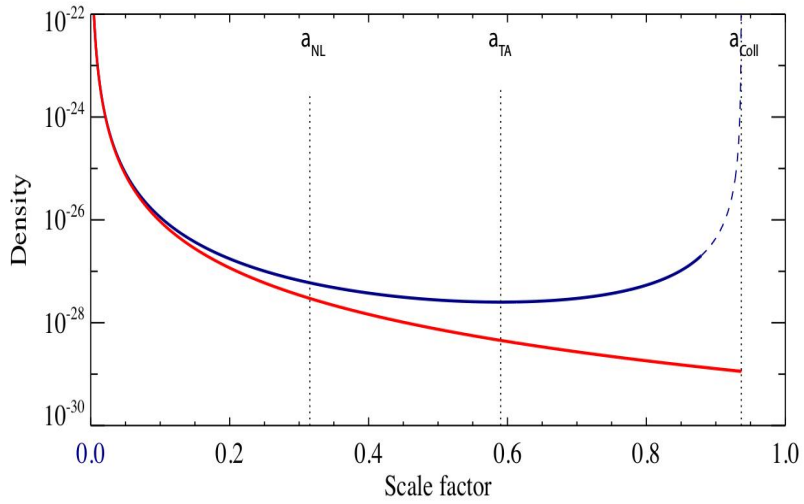

Figure 2.2: Density evolution of a spherical top-hat perturbation as a function of scale factor [12].

from spherical symmetry ensure that it doesn't collapse to a point, but virialize. Time

of the collapse, $t_{coll} = 2t_{TA}$ and from virial equilibrium condition we can show that the radius is $r_{coll} = r_{TA}/2$. The density contrast is

$$(1 + \delta_{coll}) = 18\pi^2 \approx 178. \tag{2.41}$$

These events are described in figure 2.2. Here, the red line shows the evolution of the background universe where $\rho \propto a^{-3}$. Dark blue line is same for spherical perturbation and the dashed line shows the evolution approximately after virialization. Time for turn around, non-linearity and collapse are also indicated.

2.3.1 Press-Schechter theory

The evolution of mass function of the bound objects was first proposed by Press-Schechter. Press-Schechter theory is the most used analytic formula in cosmological galaxy formation theory. The theory is based on the excursion sets of $F(\vec{r}, R_f)$, the four-dimensional initial density fluctuation field with the continuous hierarchy of filters of radii R_f. The basic idea of Press-Schechter theory is that, halos forms out of peaks in the density fluctuations. In the linearly evolved spherical collapse model, the density contrast at collapse is 1.69. Press Schechter theory assumes this correspondence till the density contrast reaches this value and then it is labeled as a collapsed halo. Hence at any time, all the regions that have a density contrast of 1.69 or higher will be in collapsed halos. Hence the fraction of mass that is in halos of mass $> M$ is given by the fraction of Gaussian distribution of RMS, σ_r that exceeds 1.69:

$$f(> M) = \frac{1}{\sqrt{2\pi}} \int_{1.69/\sigma_r}^{\infty} dx e^{-x^2/2}. \tag{2.42}$$

The fraction of mass that is in halos between M and $M + dM$ is given by df/dM. Defining $d\nu(M) = 1.69/\sigma_r$,

$$\frac{df}{dM} = \frac{1}{\sqrt{2\pi}} \frac{dx}{dM} e^{-x^2/2} \,|_{x=\nu}^{x=\infty} = \frac{1}{\sqrt{2\pi}} \frac{d\nu}{dM} e^{-x^2/2}. \tag{2.43}$$

The number density of such haloes is same as the number density of all halos (ρ_0/M) times the fraction of mass in halos from M to $M + dM$:

$$\frac{dn}{dM} = \frac{\rho_0}{M} \frac{df}{dM} = \frac{\rho_0}{M} \frac{1}{\sqrt{2\pi}} e^{-\nu^2/2} \frac{d\nu}{dM}. \tag{2.44}$$

Substituting $\frac{dlog\nu}{dlogM}=\frac{M}{\nu}\frac{d\nu}{dM}$,

$$\frac{1}{M}\frac{dn}{dM} = \frac{dn}{dlogM} = \frac{\rho_0}{M}\frac{1}{\sqrt{2\pi}}\nu e^{\nu^2/2}\left(\frac{dlog\nu}{dlogM}\right). \tag{2.45}$$

According to Press-Schechter theory, the halo mass function associated with spherical collapse can be written as:

$$\nu f(\nu) = 2\left(\frac{\nu^2}{2\pi}\right)^{1/2}\exp\left(\frac{\nu^2}{2}\right) \tag{2.46}$$

where $\nu = \delta_{sc}(z)/\sigma(m)$, the ratio of critical density for collapse to the fluctuation.

2.4 Correlation function and Power Spectrum

Galaxy correlation function in cosmology is a measure of the degree of clustering in the spatial ($\xi(r)$) or in the angular ($\omega(\theta)$) distribution of galaxies as compared to an uncorrelated homogeneous distribution. In a homogeneous distribution, the correlation function vanishes at all scales. But in the presence of inhomogeneities, the correlation is non-zero and varies with distance. Two-point correlation function gives the excess probability of one point with a certain distance 'r' from another point as compared to a random distribution of points. The Fourier transform of the two-point correlation function gives the power spectrum. Power spectrum is an important quantity that is used to characterize a random field. It is the only quantity required to completely specify a statistically homogeneous and isotropic Gaussian random field. The amplitudes of fourier components in such a field are distributed independently. Power spectrum is proportional to the root mean square amplitude. By definition, power spectrum is the Fourier transform of correlation function and these are related by the equation

$$\xi(r) = \frac{1}{2\pi^2}\int dk k^2 P(k)\frac{\sin(kr)}{kr}. \tag{2.47}$$

Where the wavenumber k and the scale or wavelength λ are related by $k = 2\pi/\lambda$. It is assumed that, fluctuations are statistically isotropic and hence we can integrate over angles in k-space. If the field we are considering is a density field, where we can draw the fluctuations from the Gaussian distribution, complete statistical distribution of the fluctuation is given by the power spectrum. Power spectrum can also be written as

$$P(k) \propto \langle|{\delta_k}^2|\rangle \tag{2.48}$$

where the averaging is over all $\hat{k}$ for a given $\mid \vec{k} \mid$ and this power per decade, $\Delta^2(k)$ is defined as

$$\Delta^2(k) = \frac{k^3 P(k)}{2\pi^2}. \tag{2.49}$$

2.5 Power spectrum of density fluctuation

The origin of initial fluctuations which lead to to the formation of structures in the universe is not completely understood. One popular explanation is that they are quantum fluctuations which are stretched up to large scales due to rapid expansion in the early universe. This phase of rapid expansion is known as inflation. The amplitude of these fluctuations on different mass scales are given by the power spectrum. Inflationary theories predict that $P(k) \propto k^n$. i.e., the primordial power spectrum has power law dependence. The scale-invariant power spectrum with spectral index $n = 1$ was proposed by Zeldovich and Harrison [13]. The fluctuations here on different scales correspond to same amplitude in gravitational potential. Most models of inflation predict $0 \leq (1 - n) \ll 1$. The growth of fluctuations on different scales can be obtained from the relation between self gravitation, pressure and damping processes. With this, the evolution of this fluctuation can be studied using tranfer function $T(k, z)$

$$P(k; z) = Ak^n T(k, z) \tag{2.50}$$

where A is the normalization factor that can be determined observationally. An important scale in the theory of gravitational collapse is the Jeans length. It is a critical radius of a gas cloud: fluctuations on scale larger than Jeans length are unstable against the contraction under gravity.

2.6 Ellipsoidal collapse

2.6.1 Zel'dovich approximation

Zel'dovich in 1970 introduced a simple approximation to describe weakly non-linear stages of structure formation. In this approximation, initial matter distribution is considered to be homogenous and collisionless. If the initial, unperturbed coordinates

(Lagrangian) of the particles are denoted by $\mathbf{q}$, the corresponding Eulerian coordinates of the particle at time t are given by

$$\mathbf{r}(\mathbf{q}, t) = a(t)[\mathbf{q} + b(t)\mathbf{s}(\mathbf{q})] \tag{2.51}$$

where $a(t)$ is the expansion factor, $b(t)$ is the growing rate of linear fluctuation given by the equation (2.25) and $\mathbf{s}(\mathbf{q})$ is the velocity term which gives the displacement of the particle with respect to its initial position. $\mathbf{s}(\mathbf{q})$ can be related to the potential $\phi(\mathbf{q})$ due to the initial density perturbations,

$$\mathbf{s}(\mathbf{q}) = \nabla\phi(\mathbf{q}). \tag{2.52}$$

Equation (2.51) can be explained as follows: let us consider a pressureless, homogeneous medium with a gravitational interaction. The relation connecting the Eulerian $\mathbf{x}$ and Lagrangian position $\mathbf{q}$ of the particles in this system at time t can be written as,

$$\mathbf{x}(\mathbf{q}, t) = \mathbf{v}(\mathbf{q})t + \mathbf{q}, \tag{2.53}$$

where $\mathbf{v}(\mathbf{q})$ is the initial velocity and $\mathbf{q}$ is the initial coordinate. Equation (2.53) is analogous to the Zel'dovich approximation (2.51) with extra factor $a(t)$ which accounts for the cosmic expansion and $b(t)$ which replaces time 't'. It can be shown that $b(t)$ is the growing solution for density contrast in linear perturbation theory [14]. At late times, there will be significant density inhomogeneities such that $\rho(\mathbf{r}, t)d^3\mathbf{r} = \rho_0 d^3\mathbf{q}$ and the density field in terms of Lagrangian coordinates is,

$$\rho(\mathbf{q}, t) = \rho_0 \mid \frac{\partial \mathbf{r}}{\partial \mathbf{q}} \mid = \frac{\bar{\rho}}{\delta_{ij} + b(t)\frac{\partial s_i}{\partial \mathbf{q}_j}}. \tag{2.54}$$

Here $\partial \mathbf{r}_i / \partial \mathbf{q}_j$ is the deformation tensor. $\bar{\rho}$ is the mean density and is equal to $\bar{\rho} = (a_0/a)^3 \rho_0$. When $b(t)s(\mathbf{q}) \ll 1$, equation (2.54) can be modified to

$$\rho(\mathbf{q}, t) \simeq \bar{\rho}[1 - b(t)\nabla_q . \mathbf{s}(\mathbf{q})], \tag{2.55}$$

which is equivalent to linear evolution. The deformation tensor is a real symmetric matrix and hence its eigen vectors actually refer to the set of three principle orthogonal axes and it can be written in terms of three eigen values $\lambda_1(q)$, $\lambda_2(q)$ and $\lambda_3(q)$ after diagonalization,

$$\rho(\mathbf{q}, t) = \frac{\bar{\rho}}{[1 - b(t)\lambda_1(q)][1 - b(t)\lambda_2(q)][1 - b(t)\lambda_3(q)]} \tag{2.56}$$

such that $\lambda_1(\mathbf{q}) \geq \lambda_2(\mathbf{q}) \geq \lambda_3(\mathbf{q})$. This ordering can be done without the loss of generality. From the nature of eigen values, it is clear that the first singularity occurs where λ attains its maximum value, let us denote it by λ_{max}. In general density is singular at $\lambda_1 = 1/b(t)$. This is the equation of a surface and hence we get sheets of infinite density in this model. Such high-density sheets are called pancakes, where contraction happens mainly along one of the three principle axes. Hence pancakes are considered to be the first structure formed during gravitational collapse. Filaments and knots are the other types of structures that form due to the contraction along two and three axes respectively [14].

2.6.2 Extended Press-Schechter theory

Press-Schechter theory works over a wide range of mass scales from dwarf galaxies to clusters, to better than a factor of two when compared with simulations. However the theory tends to systematically underpredict large mass halos and overpredict small-mass ones. In 2008, Sheth and Tormen [15] modified the standard formalism by generalizing to ellipsoidal collapse.

The gravitational collapse of homogeneous ellipsoids has been studied by many authors, ([17], [18]). Main effect of including the dynamics of ellipsoidal rather than spherical collapse is to introduce a simple dependence of critical density required for collapse on halo mass. Here the model in which the evolution of the perturbation is assumed to be better described by the initial shear field instead of density field. Initial conditions and external tides are chosen to recover the Zeldovich approximation in the linear regime and virialization is defined as the time when the third axis of the ellipsoid collapses.

In this approach, a position is randomly chosen in space and is smoothed on some scale R. Then the smoothed density is plotted as a function of R. A random trajectory is generated with steps, which are correlated and the nature of the trajectory is dependent on the smoothing filter and the nature of initial fluctuation field. This procedure is repeated for every position in space and it results in an ensemble of trajectories, each one of which starts from $\delta(R = \infty) = 0$: the universe is homogeneous on large scales. Then for each trajectory, a region of size R where the smooth density field lies above some critical density which depends on R is taken to correspond

to a collapsed halo. An object of mass $M \propto R^3$ is associated with the trajectory. Excursion set approach assumes that the mass fraction of halos will be equal to the fraction of walks which cross the threshold or the barrier for the first time when the smoothing scale is R, and is given by the following equation [19]:

$$f(R)dR = \frac{M}{\bar{\rho}} \frac{dn}{dM} dM. \tag{2.57}$$

Where dn/dM denotes the number density of halos of mass between M and $M + dM$. $(M/\bar{\rho})(dn/dM)$, denotes the mass fraction in such haloes and $\bar{\rho}$ is the background density of matter. The cosmological background model that we consider here is the Einstein-de Sitter model. The evolution of an ellipsoidal perturbation is given by three parameters, three eigen values of the deformation tensor. i.e., initial ellipticity e, prolateness p, and density contrast δ. The expansion factor at collapse as a function

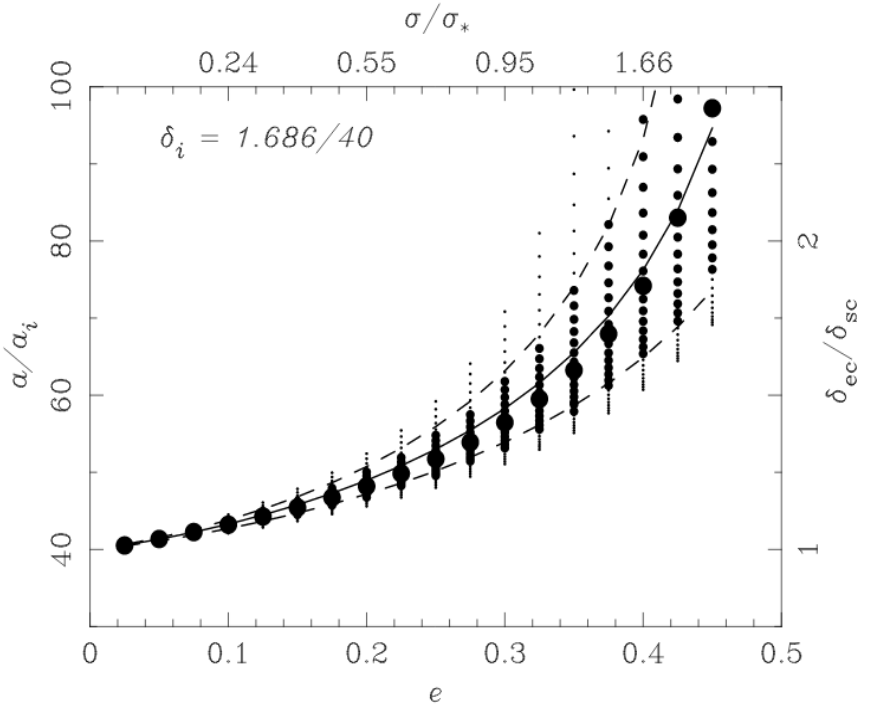

Figure 2.3: Evolution of ellipsoidal perturbation in an Einstein-de Sitter universe [15].

of e and p, for a region with initial density $\delta = 0.04215$ in Einstein-de Sitter universe is given in figure 2.3. There are three different types of circles in the figure (big, medium and small). For a given value e, the largest circles show the variation of two quantities at $p = 0$. The medium sized circles show the same at $\mid p \mid \leq e/2$, and the smallest circle show the relation at $\mid p \mid \geq e/2$. It is clear from the figure that,

virialization occurs later when e increases and for a particular value of e, it happens earlier when p decreases (given by the central line). Using this plot, equation for the threshold density contrast for ellipsoidal collapse, δ_{ec} can be constructed.

$$\frac{\delta_{ec}(e,p)}{\delta_{sc}} = 1 + \beta\left[5(e^2 \pm p^2)\frac{\delta_{ec}^2(e,p)}{{\delta_{sc}}^2}\right]^{\gamma}. \tag{2.58}$$

Where $\beta = 0.47$, $\gamma = 0.615$ and δ_{sc} is the critical density for spherical collapse. The solid curve in figure 2.3 shows the value given by equation (2.58) for $\gamma = 0.615$ and for $p = 0$ and two dashed curve shows the value for $\mid p \mid = e/2$. The goal here is to consider the collapse of ellipsoids from an initially Gaussian fluctuation field. Effect of ellipsoidal collapse in standard formalism can introduce a dependence of the critical density required for collapse on the halo mass as well as ellipticity and prolateness. We explain the approach in this section. The scatter between predicted and actual masses of halos can be reduced by using ellipsoidal collapse.

Consider a Gaussian random field smoothed on scale R_f and let $\sigma(R_f)$ be the rms fluctuation of the smoothed field. Every point in this field is associated with a perturbation potential ϕ and according to Zel'dovich approximation, second derivative of this potential is the deformation tensor. Let λ_1,λ_2 and λ_3 be the eigen values of this tensor such that $\lambda_1 \geq \lambda_2 \geq \lambda_3$. The value of different λ_i's at different positions in the smoothed field will be different. According to [20], the probability $p(\lambda_1, \lambda_2, \lambda_3)$ for eigen values is:

$$p(\lambda_1, \lambda_2, \lambda_3) = \frac{15^3}{8\pi\sqrt{5}\sigma^6}\exp\left(\frac{-3I_1^2}{\sigma^2} + \frac{15I_2}{2\sigma^2}\right) \times(\lambda_1 - \lambda_2)(\lambda_2 - \lambda_3)(\lambda_1 - \lambda_3) \tag{2.59}$$

where $\sigma \equiv \sigma(R_f)$, $I_1 = \lambda_1 + \lambda_2 + \lambda_3$, $I_2 = \lambda_1\lambda_2 + \lambda_2\lambda_3 + \lambda_1\lambda_3$ are invariants of the deformation tensor. In the linear regime, let δ be the initial density fluctuation and it is related to the potential by Poisson's equation, $\delta = I_1$. By integrating $p(\lambda_1, \lambda_2, \delta - \lambda_1 - \lambda_2)$ over $(\delta - \lambda_1)/2 \leq \lambda_2 \leq \lambda_1$ and then over $\delta/3 \leq \lambda_1 \leq \infty$, taking care of the fact that the eigen values are ordered, it is easy to show that the distribution of δ is Gaussian with σ^2 as the variance. In linear theory, $\sigma^2 \ll 1$ and $\mid \delta \mid \ll 1$. Hence the smoothing scale R_f can be associated with mass, $M \propto R_f^3$. Here, the shape of a region can be characterized by its ellipticity, e, and prolateness, p as $e = \lambda_1 - \lambda_3/2\delta$ and $p = \lambda_1 + \lambda_3 - 2\lambda_2/2\delta$. From the above relations, it is clear that the ordering of eigenvalues means that $e \geq 0$ if $\delta > 0$ and $-e \leq p \leq e$. For a spherical

region, $e = 0$ and $p = 0$. Hence the distribution of e and p for a given δ, $g(e, p|\delta)dedp$ can be written as

$$g(e, p|\delta) = \frac{1125}{\sqrt{10\pi}} e(e^2 - p^2) \left(\frac{\delta}{\sigma}\right)^5 e^{-\frac{5}{2}\frac{\delta^2}{\sigma^2}(3e^2+p^2)} \tag{2.60}$$

It can be seen that, on integrating equation (2.60) over $-e \leq p \leq e$ and then over $0 \leq e \leq \infty$ will give unity with $\delta > 0$. Value of this distribution peaks at $p = 0$ for all values of e and when $p = 0$, the maximum occurs at

$$e_{mp}(p = 0|\delta) = \frac{\sigma/\delta}{\sqrt{5}}. \tag{2.61}$$

So there is a relation between e_{mp} and σ/δ. i.e., $e_{mp} \to 0$ when $\delta/\sigma \to \infty$ which means; for a given R_f, denser regions are more likely to be spherical than less dense regions and also at a fixed δ, larger regions are more likely to be spherical than smaller ones. We can write:

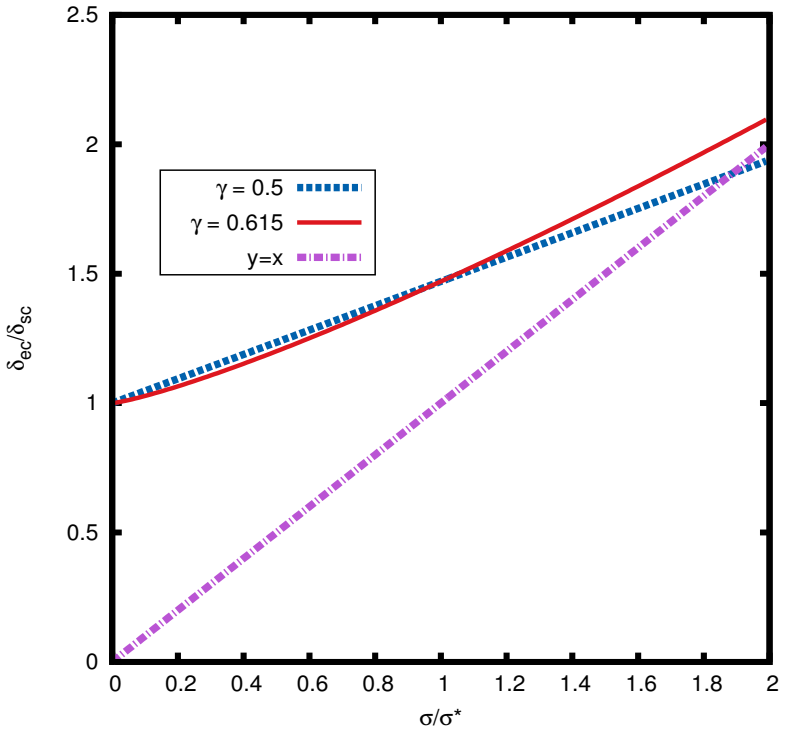

Figure 2.4: Variation of δ_{ec}/δ_{sc} and σ/σ_* with γ

.

collapse and the formation of bound objects happens when a region has an overdensity, δ_{ec} such that $e_{mp} = \left(\sigma/\delta_{ec}(e_{mp}, z)/\sqrt{5}\right)$ which means $\sigma = \sigma^2(R_f)$. i.e.,

$$e_{mp} = \frac{\sigma^2(R_f)}{\delta_{ec}(e_{mp}, z)} \frac{1}{\sqrt{5}} \tag{2.62}$$

which means $R_f^3 \propto M$ and thereby $e \propto M$, where M is the mass of halo. Also it is clear that $\delta_{ec} \propto e$. Hence it is possible to relate δ_{ec} and M as $\delta_{ec} \propto M$

$$\delta_{ec}(\sigma, z) = \delta_{sc}(z)\left(1 + \beta\left[\frac{\sigma^2}{\sigma_*^2(z)}\right]^{\gamma}\right). \tag{2.63}$$

Where we set $\sigma_*(z) \equiv \delta_{sc}(z)$. Using the above equation, it is easy to study the relation between δ_{ec} and σ with $\gamma = 0.615, 0.5$ and $\beta = 0.47$ and is shown in figure 2.4. From figure 2.4, it is clear that the value of critical density for ellipsoidal collapse increases when σ/σ_* increases. i.e., they are directly proportional. The improvement in the mass function from ellipsoidal collapse than the spherical collapse model can be seen from the graph of simulation ($M_{halo} Vs (M_{spherical}) or (M_{ellipsoidal})$) given below [15]. From this figure, we can see that, points in the panel on the right populate the

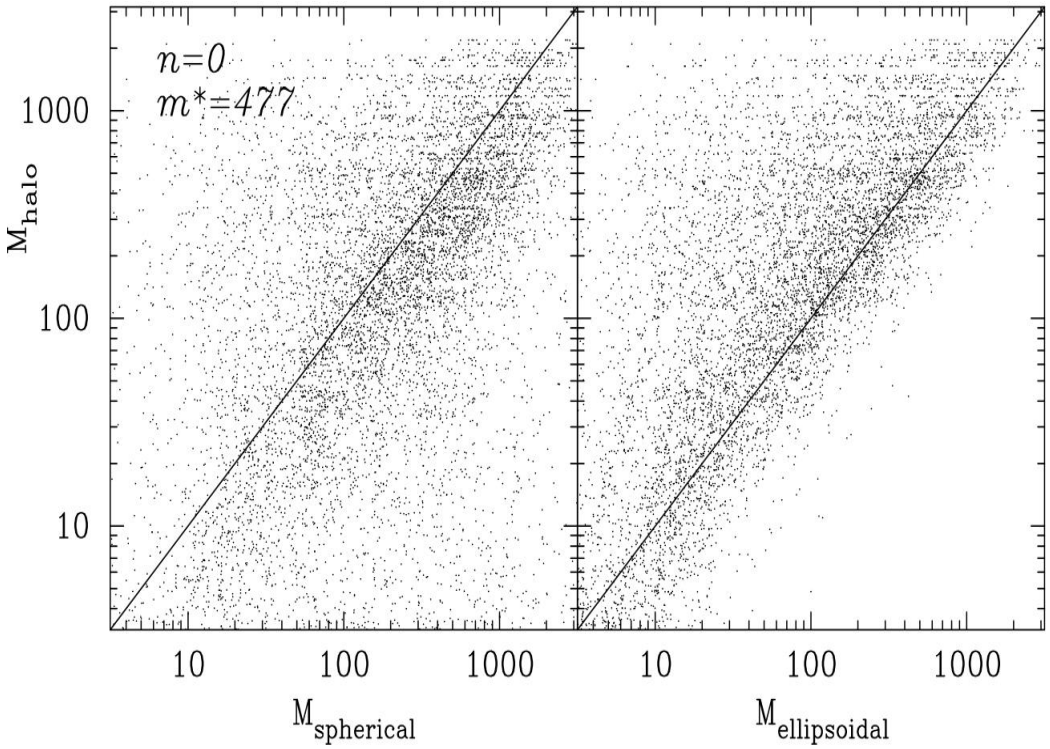

Figure 2.5: Mass of the halo, M_{halo} is plotted with the mass predicted by spherical (left panel) and ellipsoidal (right panel) collapse models [15].

upper left half only. Where, δ_{sc} is independent of the M_{halo}. Hence it is clear that the correlation between M_{halo} and $M_{predicted}$ is stronger in the ellipsoidal than in the spherical collapse model.

Finally Sheth and Tormen [15] came up with an approximation for the halo mass

function using GIF simulations, and is given by

$$\nu f(\nu) = 2A\left(1 + \frac{1}{\nu^{2q}}\right)\left(\frac{\nu^2}{2\pi}\right)^{1/2} \exp\left(-\frac{\nu^2}{2}\right) \tag{2.64}$$

where $q = 0.3$ and $A = 0.322$. While comparing GIF mass function (2.64) with the mass function obtained from the 'standard' model (2.46), we can see that they differs for $q = 0$ and $A = 1/2$.

Chapter 3

Environmental dependence

In our discussion, we have not considered the influence of environment on the collapsing halos. But in any realistic case, there will be influence of environment on the halos under consideration. This is mainly due to the large scale shear field which plays a major role. Hence there is a serious need to take it into account. In this section, we will discuss the effects of environment on halos using various properties of the tidal field.

3.1 Smoothing of fields

Excursion set approach was developed to relate the power spectrum with the abundance and clustering of non-linear structures. 'Excursion sets' refers to the sets of regions with density contrast above some threshold. Suppose we choose a random point in the initial density field. We can smooth the field around it with a filter of scale R. When we change R, the smoothed/averaged overdensity inside it will change. For very large R, the overdensity in the smoothed filter must be negligible as the universe is homogeneous on large scales. As R decreases, the overdensity will vary. Sometimes increasing and decreasing at other times. This variation can be modeled as a random walk.

In order to relate the initial density field and collapsed halos of different masses, it is important to define density field smoothed at different length scales. This can be done using window functions $W(\vec{x}, R)$. Using a window function, smoothed density

field, $\delta(\vec{x}, R)$ can be defined as

$$\delta(\mathbf{x}, R) = \int \delta(\mathbf{x}^{'}) W(\mathbf{x} - \mathbf{x}^{'}; R) d\mathbf{x}^{'} \tag{3.1}$$

In Fourier space;

$$\hat{\delta}(\mathbf{k}; R) = \hat{\delta}(\mathbf{k}) W(\mathbf{k}; R) \tag{3.2}$$

In cosmology, three window functions are used very often. Among them, most common is the spherical top-hat filter. It is defined as

$$W_{TH}(\mathbf{x}; R) = \frac{1}{V_{TH}} \begin{cases} 1 & \mid x \mid \leq R \\ 0 & \mid x \mid > R \end{cases}$$

where volume $V_{TH} = 4\pi R^3/3$. Its Fourier transform is

$$\hat{W}_{TH}(\mathbf{k}; R) = \frac{3(\sin kR - kR\cos kR)}{(kR)^3}. \tag{3.4}$$

Mass for this window function is

$$M(R) = \bar{\rho} V_{TH}(R) \tag{3.5}$$

where R is the co-moving smoothing radius and $\bar{\rho}$ is the mean matter density in the universe. It is assumed that initial density contrast is very small and may be ignored as compared to unity. In the linear regime, δ is a Gaussian random field. Variance of the smoothed field is given by:

$$\sigma^2(R) = \frac{1}{2\pi^2} \int k^3 P(k) \hat{W}(k; R)^2 \frac{dk}{k} \tag{3.6}$$

$$= \int \Delta^2(k) \hat{W}(k; R)^2 \frac{dk}{k}. \tag{3.7}$$

We sample different parts of the universe and can calculate the variance of mass contained in a volume with radius R. Mass field:

$$M(\mathbf{x}; R) = \rho(\mathbf{x}; R) V_{TH}(R) \tag{3.8}$$

where, $V_{TH}(R)$ is the volume of the window function. We have dimensionless mass variance,

$$\sigma^2(M) = \frac{1}{N} \sum \left(\frac{M(\mathbf{x}; R) - \bar{M}}{\bar{M}} \right)^2 \tag{3.9}$$

At the same time, we can write the entire mass as;

$$M(\mathbf{x}; R) = [1 + \delta(\mathbf{x}; R)]\bar{\rho}V_{TH}(R) \tag{3.10}$$

$$\bar{M} = \bar{\rho}V_{TH}(R) \tag{3.11}$$

which means

$$\frac{M(\mathbf{x}; R) - \bar{M}}{\bar{M}} = \frac{\delta M}{M} = \delta(\mathbf{x}; R) \tag{3.12}$$

From the equation (3.11) we can write

$$\sigma^2(M) = \sigma^2(R) \tag{3.13}$$

$$\sigma^2(M) = \left\langle \left(\frac{M(\mathbf{x}; R) - \bar{M}}{\bar{M}} \right)^2 \right\rangle = \int \Delta^2(k)\hat{W}(k; R)^2 \frac{dk}{k} \tag{3.14}$$

For a power-law power spectrum, $P(k) \propto k^n$

$$\sigma^2(M) \propto M^{-(n+3)/3}. \tag{3.15}$$

For $n > -3$, we can ensure that $\sigma^2(M)$ don't diverge on large scales.

3.2 Basic concepts

As we discussed in section (2.3), in case of spherical collapse, only a single parameter, density contrast is needed to fix the epoch of structure formation: the halo collapses when the linear density contrast reaches a critical threshold. Spherical approximation works well only until the first crossing. First crossing refers to the walks that first crosses δ_{sc}. This is because, Gaussian density fields are triaxial, and in the formation of non-linear structures, shear field plays a crucial role along with the density field. Ellipsoidal collapse is based on the evolution of triaxial perturbations. With the idea of the inclusion of ellipsoidal collapse conditions in the Press-Schechter approach, we have introduced a simple dependence of the critical density for collapse on the halo mass.

A recent study, [22] has indicated that halos in higher density regions form at a higher redshift for a given halo mass. Some other studies have shown that the dependence of clustering on formation time at a fixed mass is strong for halos with mass less than the characteristic mass M_* and this dependency weakens for $M > M_*$ [21]. As we

discussed in the previous section, in an ellipsoidal collapse model, the time required for virialization increases monotonically with shear. Here we discuss how the tidal force exerted by the surrounding mass distribution affects the collapse.

3.2.1 Environmental effect from the initial shear

Using the ideas discussed in sections (2.6.1) and (2.6.2), we can analyze the effects of environment on halos using different statistical properties of the initial shear.

Spectral parameter

We introduced the correlation function in section (2.4). Here we start with the two-point correlation function of the shear tensor. These functions have the following form:

$$< \xi_{ij}(x)\xi_{kl}(x) >= \frac{\gamma}{15}(\delta_{ij}\delta_{kl} + \delta_{ik}\delta_{jl} + \delta_{il}\delta_{jk}), \tag{3.16}$$

where ξ_{ij} and ξ_{kl} are the components of shear that are smoothed on different comoving scales R_0 and R_1 respectively, γ is the spectral parameter which is defined as

$$\gamma = \frac{1}{\sigma_0\sigma_1}\int_0^\infty dlnk\Delta^2_\delta(k)\hat{W}(R_0,k)\hat{W}(R_1,k) \tag{3.17}$$

and δ_{ij}'s is the Kronecker delta function, which is defined as a function of two variable such that;

$$\delta_{ij} = \begin{cases} 0 & if i \neq j, \\ 1 & if i = j. \end{cases}$$

Spectral parameter gives the strength of correlation between different scales, and is in the range $0 \leq \gamma \leq 1$. $\Delta^2_\delta \equiv k^3P_\delta(k)/2\pi^2$ is dimensionless, matter power spectrum [25]. σ_0 and σ_1 are the rms values of the density fluctuations smoothed on scales R_0 and R_1 respectively. Here onwards, we use the subscript 0 for environment and 1 for halos. γ quantifies the correlation in density field at the two scales. As mentioned earlier in section (3.1), $\hat{W}(R_i,k)$ denotes the window function at the corresponding scale R_i along with $M_i = (4\pi)/3\bar{\rho}_m R_i^3$. In this calculation, we will use top-hat filter as the window function, (3.4).

Bias

Bias gives the relation between spatial distribution of galaxies and the underlying dark matter density. So the galaxy density contrast can be written in terms of a function of underlying density contrast for matter,

$$\delta_g = f(\delta). \tag{3.19}$$

If f is a linear function of δ, we can define galaxy bias b as the ratio of the mean overdensity of galaxies to the mean over density of mass. i.e.,

$$\delta_g = b\delta. \tag{3.20}$$

Bias b depends on the luminosity, morphology, colour and redshift of the objects under consideration. In terms of correlation function, b can be defined as:

$$b = \left(\frac{\xi_{gal}}{\xi_{dm}}\right)^{1/2} \tag{3.21}$$

where b is bias of galaxies relative to dark matter and ξ_{dm} is the dark matter correlation function. Galaxy bias, $b > 1$ means: galaxies are clustered more strongly than dark matter.

Calculations

The power spectrum that we use here is a fitting function [23], where $P(k)$ is defined as

$$P(k) = \frac{Bk}{[1 + [ak + (bk)^{3/2} + (ck)^2]^\nu]^{2/\nu}}, \tag{3.22}$$

where the constants $a = (6.4/\Gamma)h^{-1}$Mpc, $b = (3/\Gamma)h^{-1}$Mpc, $c = (1.7/\Gamma)h^{-1}$Mpc and $\nu = 1.13$. We use the model with Λ, the cosmological constant. In this case with $\Lambda > 0$, $\Gamma = \Omega_m h$. Other constants are $\Omega_m = 0.3$ and $h = 0.7$. The value of B is fixed using the observed CMB anisotropies or the amplitude of fluctuations at a fixed scale like $8h^{-1}Mpc$ [17]. The power spectrum is shown in figure 3.1. We can calculate spectral parameter γ using equation (3.17). In figure 3.2, curves from top to bottom shows the correlation strength γ as a function of R_0 for five different values of R_1: $0.1, 0.5, 2, 6$ and $12h^{-1}$Mpc. These are for the model with index $n_s = 0.96$ and $\sigma_8 = 0.83$ normalisation has been done using the fitting formula given in [26]. From 3.2, we can see the dependence of environment (R_0) on the halos (R_1). Value of

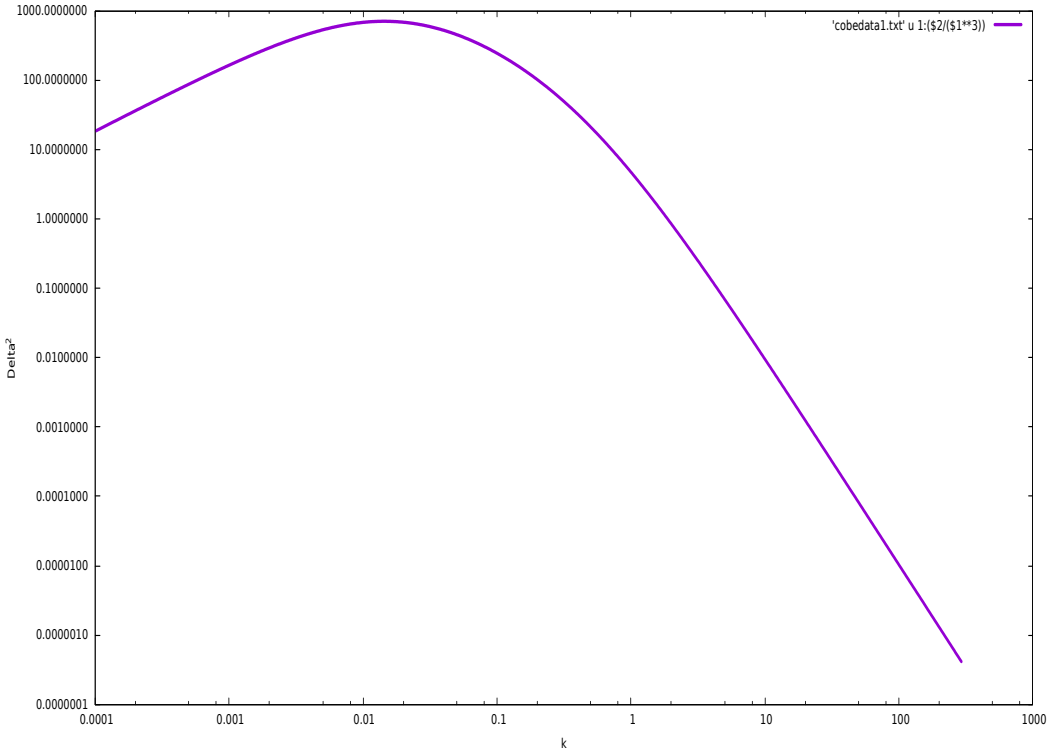

Figure 3.1: Power spectrum

.

spectral parameter decreases when the ratio R_0/R_1 increases. When it reaches unity, R_0 become equal to R_1 and the correltion between halo and environment is high. The spectral parameter decreases slowly for smaller values of R_1.

We can extend this to other cases using different power spectra. We use power law power spectra with a Gaussian cutoff and do the same calculations. The Power spectrum that we use here is,

$$P(k) = Ak^n e^{-k^2/k_0^2}. \tag{3.23}$$

Where n is the spectral index which take three values $n = -2, -1, 0$ and $k_0 = 1Mpc^{-1}$. The value of constant A is taken such that the condition $\sigma(8Mpc) = 1$ is satisfied, where $R_0 = 8$Mpc. The results that we obtained after the calculations are given below, where we can see that the same trend is followed here:

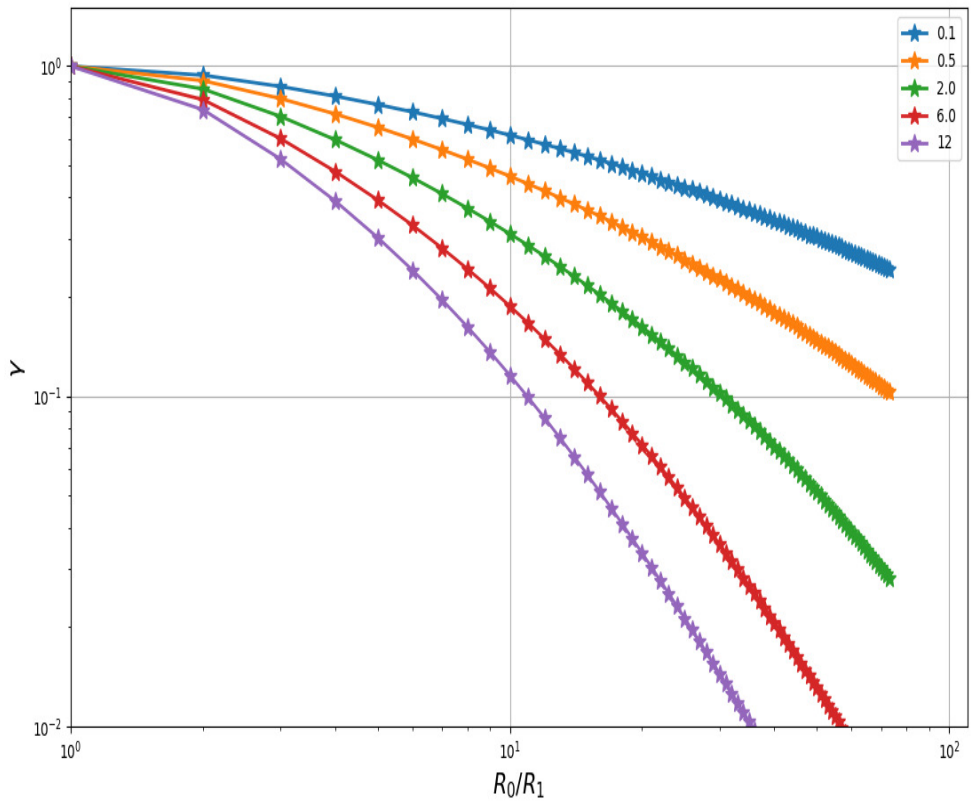

Figure 3.2: Spectral parameter γ as a function of $\frac{R_0}{R_1}$ for five values of R_1.

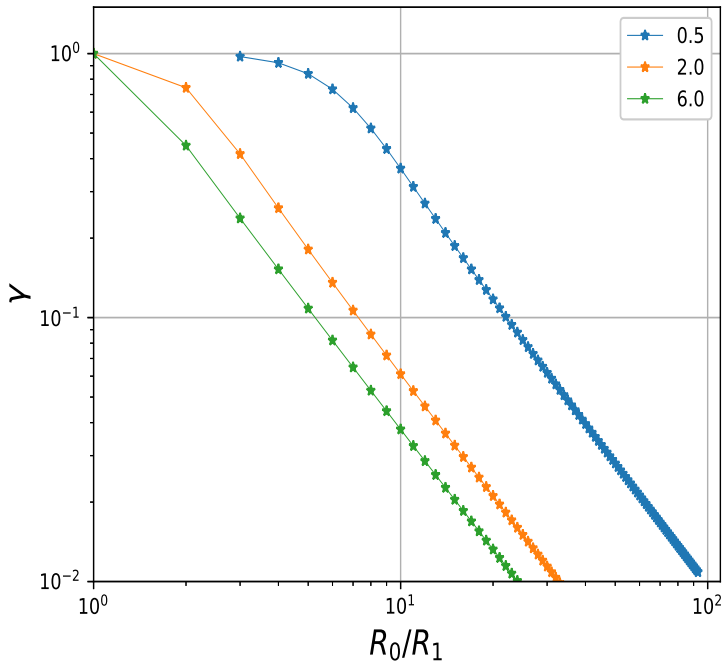

Figure 3.3: Spectral parameter γ as a function of $\frac{R_0}{R_1}$ for three values of R_1 and spectral index, $n = 0$.

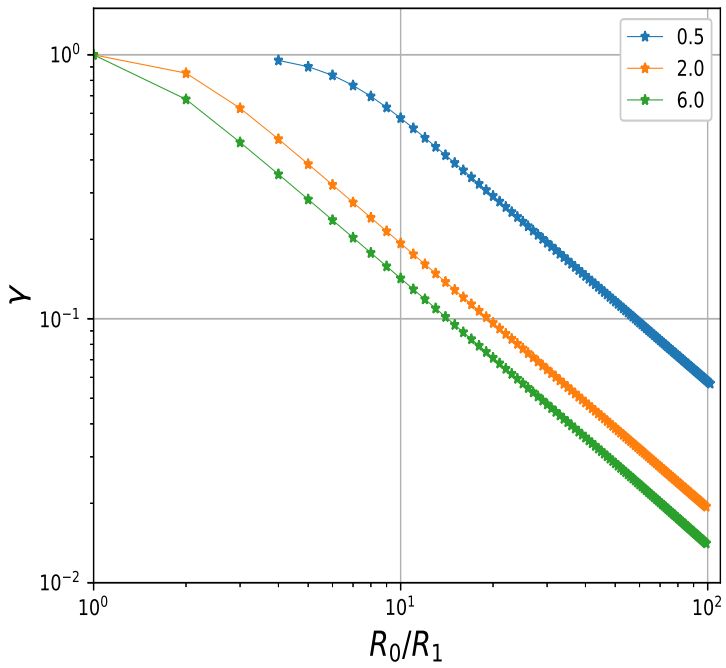

Figure 3.4: Spectral parameter γ as a function of $\frac{R_0}{R_1}$ for three values of R_1 and spectral index, $n = -1$.

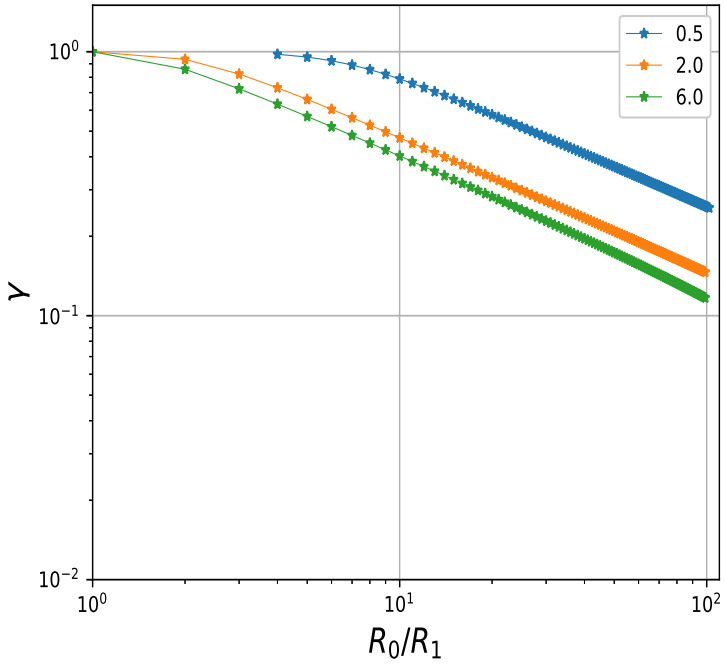

Figure 3.5: Spectral parameter γ as a function of $\frac{R_0}{R_1}$ for three values of R_1 and spectral index, $n = -2$.

Chapter 4

Conclusions

From the plots presented in the last chapter, I can make the following conclusions:

All the graphs show that, environment has effects on halos. The shear at different scales is correlated as seen from the spectral parameter γ and its variation with scale. This can be seen in case of all power spectra used here.

From figure 3.2, we can see that as the scale representing the environment, R_0 decreases, the correlation between halo and environment increases. When R_0 becomes R_1, i.e., both the environment and halo are of same scale, they are highly correlated with spectral parameter, $\gamma = 1$. In this figure, five coloured curves stand for three values of R_1. For a single value of R_0, this correlation increases as R_1 decreases.

Figures 3.3, 3.4 and 3.5 shows the same power spectrum for three different values of spectral index. Here we can see that the correlation between halo and environment is strong for small value of spectral index. It is also clear that the spectral parameter falls off faster for larger n and for a given n, the variation with scale is mainly due to the Gaussian cutoff in the power spectrum.

Bibliography

[1] White, S. D. M, Rees, M. J, Core condensation in heavy halos - A two-stage theory for galaxy formation and clustering, *Mon. Not. R. Astron. Soc.*, **183**, 341-358, 1977.

[2] White, S. D. M., Frenk, C. S, Galaxy formation through hierarchical clustering, *Astrophysical Journal*, **379**, 52-79, 1991.

[3] Michael J. Kaufman, Mark G. Wolfire, David J. Hollenbach and Michael L. Luhman, Far-Infrared and Submillimeter Emission from Galactic and Extragalactic Photodissociation Regions, *The Astrophysical Journal*, **527**, 795-813, 1999.

[4] , Gerard Lemson, Guinevere Kauffmann, Environmental Influences on Dark Matter Halos and Consequences for the Galaxies Within Them, *Mon. Not. R. Astron. Soc.*, **302**, 111-117, 1999.

[5] Marilena LoVerde, Amber Miller, Sarah Shandera1 and Licia Verde, Effects of scale- dependent non-Gaussianity on cosmological structures, *Journal of Cosmology and Astroparticle Physics*, **2008**, 1475-7516, April 2008.

[6] Michele Maggiore and Antonio Riotto, The halo mass function from excursion set theory. I. Gaussian fluctuations with non-markovian dependence on the smoothing scale, *The Astrophysical Journal*, **711**, 2-907, 2010.

[7] Press, William H.; Schechter, Paul, ormation of Galaxies and Clusters of Galaxies by Self-Similar Gravitational Condensation, *Astrophysical Journal*, **187**, 425-438, 1947.

[8] Bond J.R.; Myers S.T., The peak-patch picture of cosmic catalogs. I. Algorithms., *The Astrophysical Journal*, **103**, 1-40, 1996.

[9] Weygaert, Gaussian random fields, 2007, https://www.astro.rug.nl/ weygaert/tim1publication/lss2007/computerIII.pdf.

[10] Chapter4:linear perturbation theory, 2009, https://www.astro.rug.nl/ weygaert/tim1publication/lss2009/lss2009.linperturb.pdf.

[11] Max. Tegmark, From linear theory to galaxy formation, Sept. 13, https://ned.ipac.caltech.edu/level5/Sept13/Silk/Silk3.html.

[12] Jarle Brinchmann, Lecture 4, February 2014.

[13] V.A. Rubakov, Harrison–Zeldovich spectrum from conformal invariance, *JCAP*, **2009**, 1475-7516, 2009.

[14] The zeldovich approximation, usac.edu.gt.

[15] Ravi K. Sheth, H. J. Mo and Giuseppe Tormen, Ellipsoidal collapse and an improved model for the number and spatial distribution of dark matter halos, *Mon. Not. R. Astron. Soc.*, **323**, 1-12 , 2008.

[16] Burkhardt, G.; Esser, U.; Hefele, H.; Heinrich, I.; Hofmann, W.; Matas, V. R.; Schmadel, L. D.; Wielen, R.; Zech, G., Astronomy and Astrophysics Abstracts, *Astronomy-Astrophysics*, **68**, 1998.

[17] Peebles, P. J. E, The large-scale structure of the universe, 435, 1980.

[18] Lemson G., *Mon. Not. R. Astron. Soc.*, **263**, 913, 1993.

[19] J. R. Bond, S. Cole, G. Efstathiou and N. Kaiser, Excursion set mass functions for hierarchical Gaussian fluctuation, *The Astronomical Journal*, **379**, 440-460, 1991.

[20] Doroshkevich A. G., *Astrofizika*, **6**, 581, 1970.

[21] , Liang Gao, Volker Springel, Simon D. M. White, The age dependence of halo clustering, *Mon. Not. R. Astron. Soc.*, **363**, 66-70, 2005.

[22] Vincent Desjacques, Environmental dependence in the ellipsoidal collapse model, *Mon. Not. R. Astron. Soc.*, **388**, 638-658, (2008).

[23] G. Efstathiou, J.R. Bond and S.D.M. White, COBE background radiation and large-scale structure in the Universe, *Mon. Not. R. Astron. Soc.* **258**, 1-6, (1992).

[24] Mather et.al, A preliminary measurement of the cosmic microwave background spectrum by the Cosmic Background Explorer (COBE) satellite, *Astrophysical Journal*, **354**, L37-L40, 1990.

[25] Titouan Lazeyrasa, Christian Wagnera,b, Tobias Baldaufc and Fabian Schmidta, Precision measurement of the local bias of dark matter halos, *Journal of Cosmology and Astroparticle Physics*, **2016**, 1475-7516, 2016.

[26] Eisenstein, Daniel J.; Hu, Wayne, Power Spectra for Cold Dark Matter and Its Variants, **511**, 5-15, 1999.